

Comparison of Structural Characteristics of Straw Lignins by Alkaline and Enzymatic Hydrolysis

Di Jin,^a Weifang Dong,^a Haitao Zhang,^a Yuhui Ci,^a Lipeng Hou,^a Lihua Zang,^{a,*} Fangong Kong,^{a,*} and Lucian Lucia^b

Lignin was separated from wheat straw by NaOH cooking and enzymatic hydrolysis, obtaining yields of 86.2% and 78.6%, respectively. Fourier transform infrared spectrometry (FT-IR) and two-dimensional nuclear magnetic resonance (2D-HSQC) analyses indicated that the H units (*p*-hydroxyphenyl units) of the Enzymatic Hydrolysis Lignin (EHL) did not suffer much damage. The number-average molecular weight (M_n) of the EHL measured by gel permeation chromatography (GPC) was 3348 g/mol, which was higher than that (3047 g/mol) of Alkali Lignin (AL). The Cr(VI) adsorption experiments demonstrated that the maximum removal percentages and maximum adsorption amount of the EHL and AL were 31.5%, 88.9%, 135.1 mg/g, and 271.7 mg/g, respectively. In addition, the adsorption kinetics, adsorption isotherm and thermodynamics of Cr(VI) on these two lignins were reported in detail.

Keywords: Characteristic; Multi-enzymatic; Flocculation; Adsorption; 2D-HSQC

Contact information: a: State Key Laboratory of Biobased Material and Green Papermaking, College of Environmental Science and Engineering, Qilu University of Technology, Shandong Academy of Science, Jinan, Shandong 250353, China; b: The Laboratory of Soft Materials & Green Chemistry, Departments of Chemistry, Wood & Paper Science, North Carolina State University, Raleigh, NC 27695, USA;

* Corresponding authors: zlh@qlu.edu.cn; kfgwsj1566@163.com

INTRODUCTION

The lignins separated from raw materials or spent liquors using different separating method usually have different chemical structures and properties that contribute to their applications in different fields. In plant cell walls, cellulose, lignin, and hemicellulose are cross-linked, which promotes cell wall sturdiness (Wörmeyer *et al.* 2011). Lignin with different structure and function can be obtained by different separation methods.

Recently, enzyme technology has been applied to lignocellulose biomass pretreatment. Due to growing environmental problems, green technologies are highly valued, especially in the traditional manufacturing industries, for example the pulp and paper industry (Balea *et al.* 2017). Xylanase could remove the loose lignin by hydrolyzing the chemical bonds between lignin and hemicellulose present in the carbohydrate complex (Saleem *et al.* 2011; Nie *et al.* 2015). Laccase is an oxidase produced by white-rot fungus; it has the ability to break down lignin (Wells *et al.* 2006), and has been used in industry. Therefore, enzyme technology and its application in the pulp and paper manufacturing processes is very relevant (Menezes *et al.* 2016; Ma *et al.* 2017). The market price of enzymes has declined in the course of remarkable progress in the development of enzyme production technology that allows enzymes, such as xylanase and cellulase, to be used industrially. For example, biobleaching has been used in the pulp bleaching process and in mechanical pulping and dissolution pulping, which use enzymes (Sindhu *et al.* 2016).

Enzymology has great potential for improving pulp performance, promoting the comprehensive utilization of lignocellulosic biomass, and reducing environmental pollution (Meighan *et al.* 2017). Moreover, lignin with specific structure can be obtained due to the specific hydrolysis of plant components by enzymes.

Combinations of enzymes were used to isolate lignin from wheat straw under mild conditions, and two lignin types were separated from different cooking liquors. The properties of the two lignins were analyzed. The lignin structures and linkages between lignin and carbohydrates were investigated by two-dimensional nuclear magnetic resonance, specifically heteronuclear single quantum coherence (2D-HSQC). The *p*-coumaric acid and ferulic acid are linked to lignin and hemicellulose *via* ester and ether linkages in herbaceous plants (Scalbert *et al.* 1985, 1986; Fidalgo *et al.* 1993). The hydrolysis of lignin is nonspecific in this high temperature alkali cooking process. Alkali lignin and enzymatic hydrolysis lignin have different structures and functions.

In order to compare the difference between the enzymatic hydrolysis process and the lignin isolated by the traditional alkali cooking process, the NaOH cooking method was conducted as this method was used in non-wood pulping extensively in paper industry. This study was to compare the characteristics of straw lignins isolated by enzymatic hydrolysis and non-specific hydrolysis of traditional high temperature alkali cooking. The structural and functional characteristics of the two lignins were analyzed and discussed in order to get the difference between these two lignins as well as achieve different applications. Because lignin can adsorb heavy metals, it was used for Cr(VI) adsorption experiments. The adsorption thermodynamics and adsorption-kinetics were systematically studied. Rice straw was aminated and then grafted with polyvinyl alcohol (A-RS/PVA) to remove Cr(VI) from aqueous solution. The results showed that Cr(VI) adsorption capacity of A-RS/PVA was as high as to 140.4 mg/g at an initial pH of 2 at 60 °C (Chao *et al.* 2018). Brdar *et al.* (2012) also studied the adsorption potential of sulfate lignin on Cr(VI) ions. The present work compares the adsorption performance of alkali lignin (AL) and enzymatic hydrolysis lignin (EHL).

EXPERIMENTAL

Materials

The wheat straw came from Anhui, China. The wheat straw stems were chopped into 3 cm to 5 cm long pieces, washed 2 to 3 times with water, and air-dried. The stems were placed in sealed bags at room temperature after use. The chemical compositions (in % w/w, dry matter) of the wheat straw were determined according to the respective TAPPI standards (1996): ash (TAPPI T211 om-93), acid insoluble lignin (TAPPI T 222 om-88), acid soluble lignin (TAPPI UM 250-om-83), and pentosans (TAPPI T 223 cm-84). The cellulose content was determined by a nitric-acidic treatment method (Wright and Wallis 1998). The percentages of cellulose, hemicellulose, lignin, and ash were 35.1%, 25.8%, 20.1%, and 2.4%, respectively.

Amylase, xylanase for paper making, pectinase, and laccase were all supplied by Denykem (Shanghai, China). Lipase was purchased from Sunson (Ningxia, China). Xylanase was obtained from Sukahan (Weifang, China).

Poly-(aluminum chloride) (PAC) and polyacrylamide (PAM) were purchased from POUSET (Tianjin, China). All chemicals were analytical grade. The experiments were

conducted in a rotary lab-scale cooking system, which was processed by an electric heating cooking pot. The boiler contains four 1.5 L stainless steel reactors.

Preparations of the Enzymatic Hydrolysis Lignin and the Alkali Lignin

The wheat straw (100 g, oven-dried) was pretreated with amylase (24000 DAU/G sample, 0.4 g) for 30 min at 120 °C at a ratio of deionized water to straw of 5:1 (v/w). Then the mixtures were treated with sodium hydroxide (6% based on oven-dried straws) at 120 °C for 2 h. Next, the temperature was decreased to 95 °C and cooked for 1 h with 27 mL of 30% H₂O₂. The xylanase for paper making (1500 TXU/g sample, 0.9 g) was added and cooked at 95 °C for 1 h. When the temperature was decreased to 65 °C, pectinase (20000 DPU/G sample, 0.3 g) and xylanase (80000 U/g sample, 0.3 g) were added to react for 1 h. Finally, the cooked mixture was cooled to 45 °C and insulated for 16 h with laccase (5000 DLU/G sample, 0.6 g) and lipase (100 U/mg, 0.5 g). After cooking, the solids and liquids were separated. The solids were washed until the filtrate was colorless and then deposited in a sealed bag at 4 °C for later use. The EHL was separated from the liquid by dilute sulfuric acid precipitation to a pH of 2.0 under stirring conditions (Yuan *et al.* 2009). Each run was repeated at least three times to ensure good reproducibility. The lignin yield was calculated by Eq. 1,

$$\text{Yield (\%)} = \frac{\text{Mass of the separated lignin}}{\text{Mass of the lignin in the initial dry samples}} \times 100\% \quad (1)$$

Additionally, the wheat straw was mixed with 18% NaOH ($W_{\text{NaOH}}/W_{\text{oven dried straw}}$) solution, and the liquid to solid ratio was 5:1 (v/w). The commixtures were heated to 160 °C and kept for 90 min. Next, the AL was obtained by treating the liquid and residue as described above.

Characterization

Some functional groups of lignin were determined by Fourier-transform infrared spectrometer (FT-IR) (IR prestige-21, Shimadzu, Japan). Potassium bromide was milled with samples at a mass ratio of 100 mg/1 mg. The scanning wave number ranged from 4000 cm⁻¹ to 400 cm⁻¹, and 64 scans were performed with a 2 cm⁻¹ resolution.

Gel permeation chromatography (GPC) (model PL-GPC50, Agilent Technologies, Santa Clara, USA) was used to determine the molecular weight of the two lignins. The two samples and N,N-dimethylformamide (DMF) were mixed at a ratio of 1:1 (mg/mL), respectively. A total of 25 µL of the DMF solutions were filtered by a 0.45 µm filter and injected in the GPC column with DMF eluant (1.0 mL/min) at 40 °C for analysis.

To examine the structure of the two lignins in further detail, an AVANCEIIIHD 500MHz instrument (Bruker, Fällanden, Switzerland) was used to obtain the NMR spectra of lignin in solution at 25 °C. Next, 80 mg of samples were dissolved in 0.5 mL with DMSO-*d*₆ (99.8%) for the experiments. The HSQC experimental mode was used to collect data (Sun *et al.* 2016). The parameters were as follows: pulse width (9.2 µs), the pulse angle (30°), acquired time (3.28 s), and delay time (1.00 s). MestReNova software (beta) (Mestrelab Research, Santiago de Compostela, Spain) was used to analyze 2D profiles in all the spectra (Yang *et al.* 2016). The two lignins were semi-quantitatively analyzed by 2D-HSQC NMR spectra (Zikeli *et al.* 2016).

X-ray photoelectron spectroscopy (XPS) was used to study the adsorption mechanism of lignin samples. An Al Ka X-ray source at 1486.6 eV was used in the XPS

analysis. Binding energy values were calibrated using characteristic carbon (C1s = 284.8eV) during data processing of XPS spectra.

Surface areas of the two lignins were estimated by quantachrom NOVA 1000 surface area analyzer, with N₂ at 77 K.

Comparison of Cr(VI) Adsorption Properties of the EHL and the AL

Adsorptive removal

Under batch conditions, the removal efficiency of Cr(VI) from aqueous solution by the two lignins was determined. 50 mL of Cr(VI) solutions with different initial concentrations (100 to 300 mg/L) and a pH of 2 were mixed with the lignins at a 0.5 g/L concentration. The mixtures were added to a 100 mL conical flask and shaken at (288 K to 318 K) and 100 rpm for different contact times (0 to 12 h). After the contacted, the samples were filtered and measured with an Ultraviolet visible spectrophotometer with a wavelength of 540 nm. Each experiment was repeated three times, and the removal percentage of Cr(VI) was calculated according to the following Eq. 2,

$$\text{Removal percentage (\%)} = \frac{C_0 - C_e}{C_0} \times 100\% \quad (2)$$

where C_e and C_0 (mg/L) are the equilibrium and initial concentrations of the Cr(VI) solution, respectively.

Adsorption isotherms

Cr(VI) solutions with different initial concentrations (100 mg/L to 300 mg/L) were placed in a series of conical flasks of 100 mL for adsorption experiments to determine the equilibrium isotherm of the EHL and the AL adsorption. The experiment was divided into two groups, the first group was treated with the EHL, and the second group was treated with the AL. At different temperatures (288 K to 318 K), it was placed in a 100 rpm shaking table, with a pH of 2, and a 0.5 g/L lignin concentration for 12 h. The concentration of the Cr(VI) solution was determined, and the balance adsorption capacity q_e (mg/g) of each ingredient under equilibrium was calculated as follows,

$$q_e = \frac{(C_0 - C_e)V}{W} \quad (3)$$

where W (g) and V (L) are the weight of lignin and the volume of the solution, respectively.

The experimental isotherm data of lignin adsorption on Cr(VI) were fitted using Langmuir (1916) and Freundlich equations (Ahmed and Theydan 2012). These equations can be written as follows (Zhang *et al.* 2019),

$$\text{Langmuir isotherm } \frac{C_e}{q_e} = \frac{1}{q_m K_L} + \frac{1}{q_m} C_e \quad (4)$$

$$\text{Freundlich isotherm } \ln q_e = \ln K_F + \frac{1}{n} \ln C_e \quad (5)$$

where q_m (mg/g) is the maximum absorption of the Langmuir per unit mass of lignin to Cr(VI), K_L (L/mg) is the constant associated with the adsorption rate of the Langmuir, and K_F ((mg/g) (L/mg)^{1/n}) and n are Freundlich constants, which can be used to measure the adsorption capacity and adsorption strength of the lignin.

Adsorption kinetics

During the kinetic adsorption experiment, water samples were taken at regular times and the Cr(VI) concentration was measured. The adsorption quantity q_t (mg/g) of Cr(VI) at time t (h) was computed by Eq. 6,

$$q_t = \frac{(C_0 - C_t)V}{W} \quad (6)$$

where C_t (mg/L) is the concentration of the Cr(VI) solution at time t (h). The pseudo-first order model (Ahmed and Theydan 2012) and pseudo-second order model (Ho and McKay 1999) were calculated as follows,

$$\text{Pseudo-first order model } \ln(q_t - q_e) = \ln(q_e) - K_1 t \quad (7)$$

$$\text{Pseudo-second order model } \frac{t}{q_t} = \frac{1}{K_2 q_e} + \frac{t}{q_e} \quad (8)$$

where q_t and q_e (mg/g) are the uptake of Cr(VI) at time t (h) and at equilibrium, respectively, K_1 (1/h) is the constant quality of adsorption rate, K_2 (g/mg h) is the second-order equation rate constant.

Adsorption thermodynamics

The adsorption thermodynamic behavior of the lignins on Cr(VI) was assessed with the thermodynamic parameters by incorporating the change in enthalpy (ΔH), free energy (ΔG), and entropy (ΔS). These thermodynamic parameters are computed by the following equations,

$$\ln(K_d) = \frac{\Delta S}{R} - \frac{\Delta H}{RT} \quad (9)$$

$$\Delta G = -RT \ln(K_d) \quad (10)$$

$$K_d = \frac{q_e(W/V)}{C_e} \quad (11)$$

where K_d is the distribution coefficient, R is the general gas constant (8.314 J/mol K), and T is the temperature (K).

RESULTS AND DISCUSSION**Lignin Yields**

The yields of the EHL and the AL were 78.6% and 82.6%, and the purity was 90.6% and 87.5%, respectively, as shown in Table 1. This was calculated by Eq. 1 and NREL (National Renewable Energy Laboratory) experiment method (Sluiter *et al.* 2008).

Table 1. Alkali Lignin and Enzymatic Hydrolysis Lignin Yields and Purity

Samples	Yield (%)	Klason Lignin (%)	Acid-soluble Lignin (%)	Purity (%)
Enzymatic Hydrolysis Lignin	78.62	88.44	2.2	90.64
Alkali Lignin	86.21	82.87	4.61	87.47

Experiment on the Flocculation of the Two Liquids

The flocculation experiments were carried out on two kinds of liquids, as shown in Fig. 1. Figures 1e and 1h correspond to the alkali cooking solutions, whereas Figs. 1f and 1g are for the enzymatic hydrolysates. Poly-(aluminum chloride) (PAC) and polyacrylamide (PAM) flocculants were added to the two liquids to test their optimal flocculation performance and determine the optimal flocculation conditions. 30 mL of the alkali cooking liquid and the enzymatic hydrolysis liquid, which had been adjusted to similar chemical oxygen demand as well as the pH at 8.0, were firstly placed in a test tube and then the required amount of PAC and PAM were added into the solutions. After turning the tube up and down three times by hand, the tube was then kept statically at room temperature for different time periods to see the flocculation performance. Previous studies have shown that the color of the liquid is mainly related to the dissolved lignin. The flocculation effects of two kinds of liquids were different completely. As shown in Fig. 1, the flocculating substance in enzymatic hydrolysate was floating, and another was sediment. The factors influencing flocculation were related to the flocculant dosage, molecular weight of solute, and so on. It could be concluded from the experimental phenomenon that the molecular weight of the AL was smaller than that of the EHL, which was also confirmed by GPC. In addition, carbonate compounds would be likely formed in the enzymatic hydrolysis process, and CO₂ could be produced, which would contribute to the substances floating.

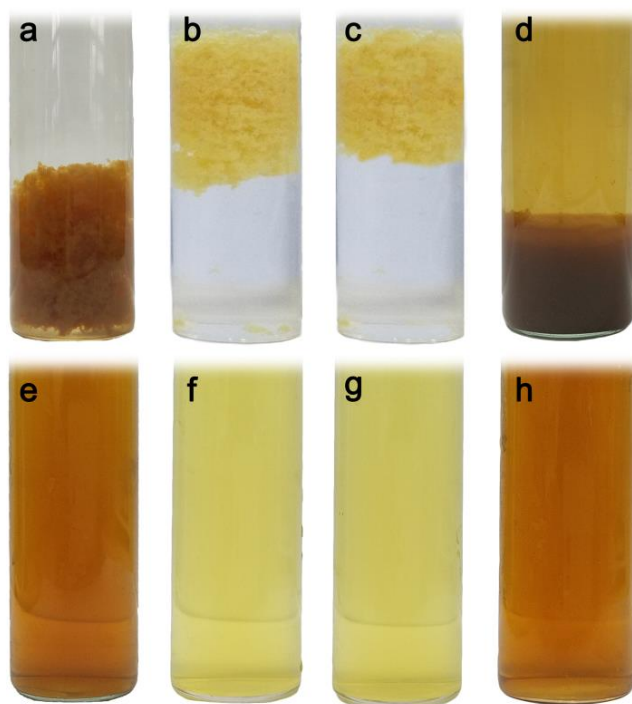


Fig. 1. The flocculation effect of the alkali lignin and the enzymatic hydrolysis lignin (a) Flocculation of alkali cooking liquid at pH= 8, PAM 2.7×10^{-4} g/L, PAC 1.35×10^{-3} g/L, and 15 min; b) Flocculation of enzymolysis liquid at pH= 8, PAM 2.7×10^{-4} g/L, PAC 1.35×10^{-3} g/L, and 15 min; c) Flocculation of enzymolysis liquid at pH= 8, PAM 6×10^{-5} g/L, PAC 3×10^{-4} g/L, and 25 min; d) Flocculation of alkali cooking liquid at pH= 8, PAM 6×10^{-5} g/L, PAC 3×10^{-4} g/L, and 25 min; e) and h) Alkali cooking liquid; f) and g) Enzymatic hydrolysis liquid

FT-IR Analysis

The functional groups and structures of the two lignins were observed by infrared spectroscopy. The characteristic signals at 1600, 1500, and 1428 cm^{-1} are related to aromatic skeleton vibration, suggesting that the aromatic structure of lignin did not altered significantly in these two processes (Li *et al.* 2012). As shown in Fig. 2, the absorption intensity of EHL at the peaks of 834, 1126, 1329, and 1651 cm^{-1} was stronger than that of AL. The spectral peak at 1126 cm^{-1} was assigned to the C-H vibration of the syringyl aryl unit (S). The band at 1329 cm^{-1} pertained to the syringylaromatic units of C=O stretching (Singh *et al.* 2005). The signal intensity of p-hydroxyphenyl unit (H) at 834 cm^{-1} was reduced in spectrum of AL compared with that of enzymatic hydrolysis lignin, which indicated that parts of H-type lignin were damaged during the alkaline cooking via ester hydrolysis (Ying *et al.* 2018). An unconjugated carbonyl group was attributed to the stretching at 1715 cm^{-1} , the stretched band at 1630 cm^{-1} was caused by the carbonyl group, and 1510 cm^{-1} was vibrated by aromatic skeleton (Toledano *et al.* 2010). In the lignin spectra, the band at 1230 cm^{-1} was C-O stretching with a guaiacyl ring (G). The figure at 1329 cm^{-1} was due to a guaiacyl-propane ring (G) and a syringyl-propane ring (S) (Faix 1991). Based on these findings, it could be concluded that the main substructures of the two lignins were H-G-S type.

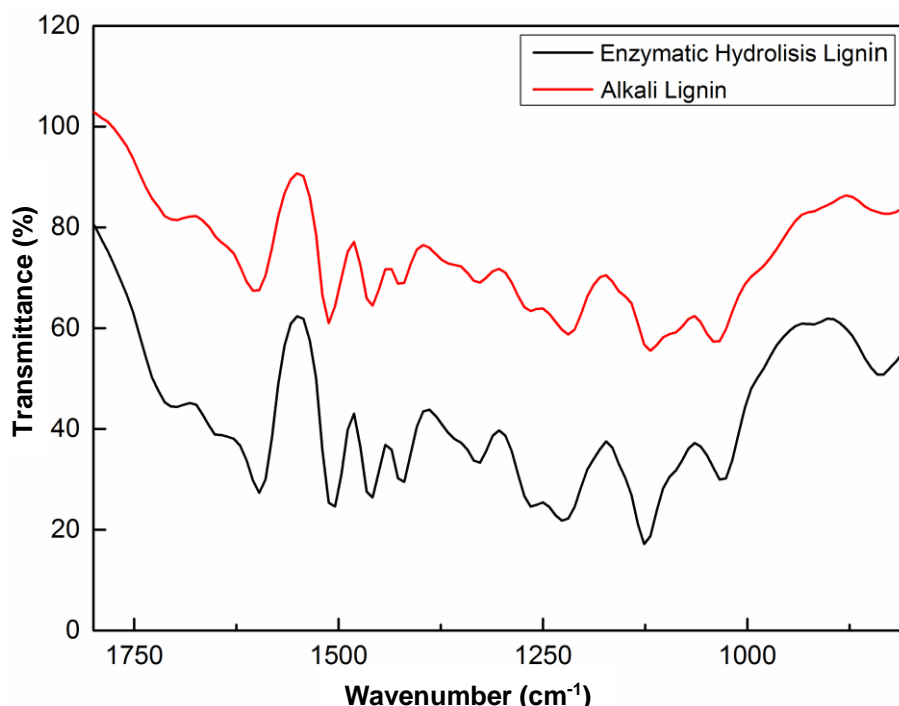


Fig. 2. FT-IR spectroscopy of the alkali lignin and the enzymatic hydrolysis lignin

Molecular Weight Analysis of the Lignin

The number-average molecular weight (M_n), the weight-average molecular weight (M_w), and the polydispersity of the two lignins are shown in Table 2. As shown in Table 2, the molecular weight and the M_w/M_n of these two lignins are different. The enzymatic hydrolysis lignin has higher molecular weight and polydispersity than alkali lignin. The data in Table 2 also shows that these two lignin samples did not have wide distributions of mass.

The molecular weight of AL in this study was higher than that reported by Zikeli *et al.* (2016). The molecular weight of lignin is a fundamental factor affecting the properties of lignin (Tolbert *et al.* 2014), which also indicate these two lignins have different potential application.

Table 2. Number-average Molecular Weights (M_n), Weight-average Molecular Weights (M_w), and (M_w/M_n) of the Two Lignins

Sample	M_w (g/mol)	M_n (g/mol)	M_w/M_n
Alkali Lignin	4053	3047	1.33
Enzymatic Hydrolysis Lignin	5226	3348	1.56

2D-HSQC

A two-dimensional nuclear magnetic resonance (2D-HSQC) NMR analysis of the EHL and AL was carried out, and the signals were based on previous literature (Balakshin *et al.* 2011; Yang *et al.* 2014; Sasaki *et al.* 2015; Zhao *et al.* 2018). The relevant signals of the aromatic/unsaturated areas (δ_C/δ_H 95 to 135/5.7 ppm to 8.0 ppm) and the side chain areas (δ_C/δ_H 50 to 95/2.5 ppm to 5.7 ppm) are shown in Fig. 3. The main correlation peaks of lignin in the 2D-HSQC NMR spectrum are listed in Table 3.

Table 3. Distributions of Peak Values in 2D-HSQC NMR Spectrum of Enzymatic Hydrolysis Lignin and Alkali Lignin

Label	$\bar{\delta}_C / \bar{\delta}_H$ (ppm) ^a	$\bar{\delta}_C / \bar{\delta}_H$ (ppm) ^b	Assignments
B_β	53.45/3.48	ND*	C_β - H_β in phenylcoumaran substructures
OCH ₃	56.17/3.14	56.18/3.15	C-H in methoxyls
A_γ	60.4/3.21	59.64/3.38	C_γ - H_γ in γ -hydroxylated β -O-4 substructures (A)
A'_γ	63.41/3.66	63.56/3.89	C_γ - H_γ in γ -hydroxylated β -O-4' substructures (A')
F_γ	61.97/4.12	61.95/4.11	C_γ - H_γ in cinnamyl alcohol end-groups (F)
X_5	70.18/3.52	ND	C_5 - H_5 in β -D-xylopyranoside (X_5)
A_α	72.39/4.87	ND	C_α - H_α in β -O-4 substructures (A)
A_β (S)	86.41/4.12	86.68/3.99	C_β - H_β in β -O-4 substructures linked to a S-unit (A)
X_3	ND	74.4/3.26	C_3 - H_3 in β -D -xylopyranoside (X_3)
X_4	ND	75.8/3.52	C_4 - H_4 in β -D-xylopyranoside (X_4)
$S_{2,6}$	104.6/6.72	104.06/6.61	$C_{2,6}$ - $H_{2,6}$ in syringyl units (S)
$S'_{2,6}$	107.2/7.25	106.59/7.24	$C_{2,6}$ - $H_{2,6}$ in syringyl units (S')
G_2	111.66/7.01	112/6.7	C_2 - H_2 in guaiacyl units (G)
G_5	115.43/6.7	115.67/6.69	C_5 - H_5 in guaiacyl units (G)
G_6	119.53/6.84	119/6.5	C_6 - H_6 in guaiacyl units (G)
FA_6	122.7/7.11	ND	C_6 - H_6 in ferulate (FA)
$H_{2,6}$	128/7.2	128.38/7.06	$C_{2,6}$ - $H_{2,6}$ in p -hydroxyphenyl units ($H_{2,6}$)
$pCA_{2,6}$	130.28/7.54	ND	$C_{2,6}$ - $H_{2,6}$, p -coumaroylated substructures (pCA)
pCA_α	144.54/7.51	ND	C_α - H_α , p -coumaroylated substructures (pCA)

^a and ^b on behalf of the peak values specified in 2D HSQC NMR spectrum of enzymatic hydrolysis lignin and alkali lignin, respectively.

*ND: not detected

As shown in Fig. 3, strong signals corresponding to β -O-4 bonds and -OCH₃ groups (δ_C/δ_H 56.3/3.69 ppm) were observed. β -5 structure was not observed in alkali lignin, which may be because the 2D-HSQC NMR resolution of the condensed lignin was reduced, making the low detection probability of β -5 structure.

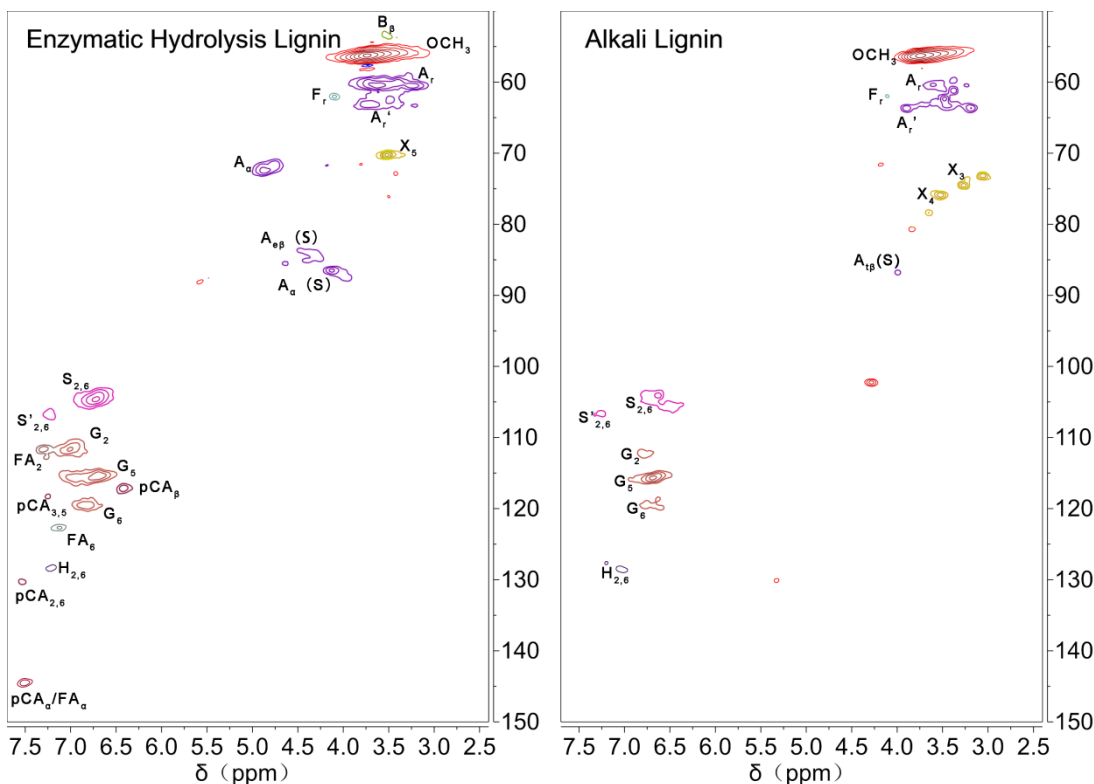


Fig. 3. 2D-HSQC NMR spectra of EHL and AL (G) guaiacyl units, (S) syringyl units, (H) *p*-hydroxyphenyl units, (pCA) esterified *p*-coumaric acid, (FA) esterified ferulic acid, (A) β -O-4 alkyl-aryl ethers, (A') β -O-4 alkyl-aryl ethers with acylated γ -OH, and (F) cinnamyl alcohol end-groups

Semi-quantitative analysis was applied in this study. The content of the H unit was relatively low compared to the amounts of the G and S units in these two lignins. AL and EHL had different monomer composition, and alkali lignin had more G units than S units, while enzymatic lignin had the opposite, as shown in Table 4.

Table 4. Monomeric Ratio and Different Inter-unit Linkages of Enzymatic Hydrolysis Lignin and Alkali Lignin

Lignin fraction	Monomeric Ratio (%)			Interunit Linkages (%)		
	S units	G units	H units	β -O-4	β - β	β -5
EHL	60.61	36.44	2.95	90.58	8.55	0.87
AL	36.23	62.42	1.35	96.88	3.13	0

In addition, the content of the H unit of both lignins was relatively low. Compared with the content of H unit of enzymatic lignin, the content of the H unit of alkali-lignin was relatively low. The only signals for xylose units without acetyl groups (X₃, X₄, and X₅) were detected for the EHL and the AL fractions, indicating the presence of different xylan structures in the two fractions. As shown in Table 3, the ferulate acid (FA (δ_C/δ_H

122.7/7.11)) and *p*-Coumaric acid (*p*CA (δ_C/δ_H 130.28/7.54, 144.54/7.51)) were found in the EHL, but they were not found in the AL. This indicated that carbohydrates were mainly hydrolyzed in the enzymatic hydrolysis process, whereas *p*CA and FA were well retained in the lignin. The strong alkaline process mainly contributed to the cleavage of chemical bonds in the lignin molecule and the cleavage of ester groups between lignin and carbohydrates. Ferulate acid and *p*-coumaric acid are important components of lignin-carbohydrates, which link lignin to carbohydrates via ether and ester linkages, respectively (Buranov and Mazza 2008). It could be concluded that the lignin was susceptible to degradation during the strong base treatment process.

Adsorption Test

Effect of the contact time

Based on the experimental design of the cited work on Cr(VI) adsorption (Albadarin *et al.* 2011), the single-factor experiments on pH, temperature, time and dosage were carried out respectively to optimize the adsorption conditions. Here, only the effect of the contact time (0 h to 12 h) on Cr(VI) removal percentages at the same initial concentrations is presented in Fig. 4. As shown, the removal rate increased when the adsorption time increased. The maximum Cr(VI) removal percentages of the EHL and the AL were 31.5% and 88.9%, respectively, at 298 K, pH of 2, and 0.5 g/L lignin concentration. On this basis, the adsorption kinetics, adsorption isotherm, thermodynamics and other experiments were carried out.

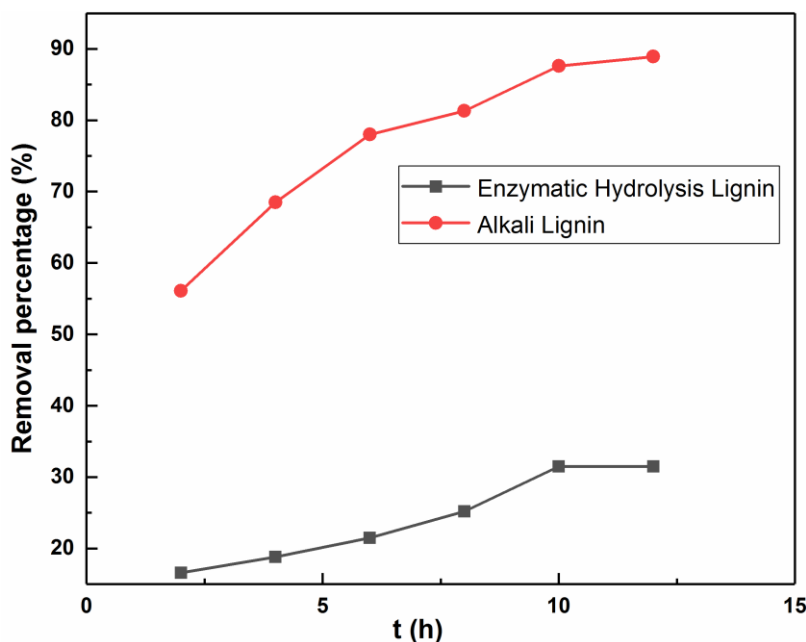


Fig. 4. Effect of the contact time on the removal percentage of Cr(VI) at 298K (pH of 2, 0.5 g/L lignin concentration)

Adsorption isotherms

The Cr(VI) adsorption test was carried out at 298 K and at different initial concentrations. The removal efficiency of Cr(VI) in the solution was calculated with Eq. 2. The Langmuir and Freundlich isotherms were fitted with Eqs. 4 and 5, respectively, and the calculated constants from the two isotherm equations for both components are presented in Table 5. The maximum adsorption capacity of the AL and the EHL on Cr(VI)

at 298 K by the Langmuir isotherm was 271.7 mg/g and 135.1 mg/g, respectively. Table 5 shows that the Langmuir isotherm ($R^2 = 0.854$) was more suitable than the Freundlich isotherm ($R^2 = 0.638$) to describe the adsorption of the enzymatic lignin on Cr(VI), indicating that the adsorption was single-layer adsorption. According to Langmuir's calculation, the maximum adsorption capacity under this condition was 135.1 mg/g. At the same time, the Langmuir isotherm ($R^2 = 0.986$) was more suitable than the Freundlich isotherm ($R^2 = 0.845$) to describe the adsorption of the AL on Cr(VI). To verify if the Cr(VI) was adsorbed on the lignin surface, the XPS was used to determine the existence of Cr ions on the lignin surface. As shown in Fig. 5, the two peaks at 586.1 eV and 576.3 eV representing ionic compounds of Cr(III) and Cr(VI) were found in the spectra of both enzymatic hydrolysis lignin and alkali lignin respectively, which indicated that Cr(III) and Cr(VI) were present on the lignin after adsorption. The appearance of Cr(III) peak at 586.1 eV indicated that some Cr(VI) was reduced to Cr(III) under the acidic conditions applied in this experiment.

Table 5. Adsorption Isotherm Analysis of Cr(VI) Adsorption by EHL and AL

Adsorbent	Freundlich			Langmuir		
	K_F	n	R^2	q_m (mg/g)	K_L	R^2
Enzymatic Hydrolysis Lignin	14.8	2.91	0.638	135.1	0.67	0.854
Alkali Lignin	15.98	3.52	0.845	271.7	0.002	0.986

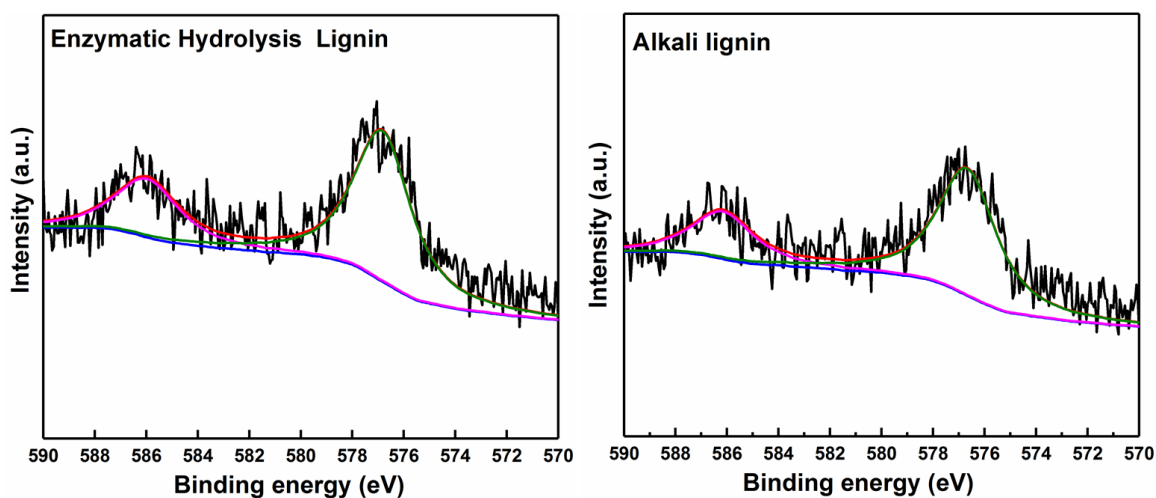


Fig. 5. XPS analysis of EHL and AL after adsorption of Cr(VI)

Adsorption kinetics

Table 6 shows the kinetic adsorption fitting results of Cr(VI) by the two lignins. The R^2 (0.978/0.988) value of the pseudo-second order kinetic analysis of both lignins was greater than (0.922/0.948), that of the pseudo-first order. Moreover, $q_{e,exp}$ was in accordance with $q_{e,cal}$. Therefore, the pseudo-second-order could be used to analyze the chemical adsorption of Cr(VI) by the two lignins. Table 6 showed that the rate constant of the EHL was greater than that of the AL, which may be because the adsorption capacity of the AL was higher than that of the EHL. The specific surface area of these two lignins has been determined, being 5.31 m^2/g , and 6.79 m^2/g of EHL and AL, respectively.

Table 6. Kinetic Analysis of Cr(VI) Adsorption by EHL and AL

Adsorbents	$q_{e,exp}$ (mg/g)	Pseudo-first order model			Pseudo-second order model		
		$q_{e1,cal}$ (mg/g)	K_1	R^2	$q_{e2,cal}$ (mg/g)	K_2	R^2
Enzymatic Hydrolysis Lignin	63	4.62	0.033	0.922	45.45	0.048	0.978
Alkali Lignin	180.09	8.3	0.126	0.948	189.75	0.0057	0.988

Table 7. Adsorption Thermodynamics Parameters

Adsorbents	$1/T(K^{-1})$	$\ln K_d$	ΔH (KJ/mol)	ΔS (J/mol)	ΔG (KJ/mol)
Enzymatic Hydrolysis Lignin	0.00347	2.597	34.36	141.43	-6.22
	0.00335	3.172			-7.86
	0.00325	3.722			-9.53
	0.00315	3.908			-10.33
Alkali Lignin	5.60876	5.609	43.55	126.31	-13.43
	6.16104	6.161			-15.26
	6.78859	6.789			-17.38
	6.99357	6.994			-18.49

Adsorption thermodynamics analysis

Equations 9 through 11 were fitted to the experimental data of $1/T$ in (K_d), and the thermodynamic parameters of lignin were used (Table 7). The Gibbs free energy was negative, which indicated the thermodynamic spontaneity of the adsorption. As the temperature increased, the ΔG values increased, indicating the feasibility of adsorption as the temperature increases. The value of ΔH was an indicator of the endothermic or exothermic properties, and its value provided information about the adsorption type, which could be chemical or physical. The physical adsorption was in line with the adsorption enthalpy range of 2.1 kJ/mol to 20.9 kJ/mol (Saha *et al.* 2010). The heat of adsorption of Cr(VI) by EHL and AL was not in this range, so it belonged to chemical adsorption.

CONCLUSIONS

1. The alkali lignin (AL) yield was 86.2%, which was higher than that (78.6%) of the enzymatic hydrolysis lignin (EHL). The flocculation effect of the two liquids was different, in which the flocculated lignin was floating in the upper phase in the enzymatic hydrolysis liquid, and the flocculated lignin was precipitated at the bottom in the alkali cooking liquid.
2. The FTIR and 2D-NMR spectra indicated that the S and G units in the EHL were not severely damaged compared with the AL. The molecular weight (3348 g/mol) of the EHL was higher than that (3047 g/mol) of the AL.
3. The equilibrium adsorption data of lignin for Cr(VI) at 298 K was well fitted to the Langmuir isotherm model. The maximum adsorption capacities and Cr(VI) removals of the EHL and the AL were 135.1 mg/g, 271.7mg/g, and 31.5% and 88.9%, respectively, at the conditions of 298 K, pH of 2, and 0.5 g/L lignin concentration. The XPS indicated that Cr(VI) was present and was adsorbed by the lignins.

ACKNOWLEDGEMENTS

The authors are grateful for the National Key R&D Program of China (No. 2017YFB0308000) and National Natural Science Foundation of China (Grant Nos. 31570566).

REFERENCES CITED

- Ahmed, M. J. and Theydan, S. K. (2012). "Equilibrium isotherms, kinetics and thermodynamics studies of phenolic compounds adsorption on palm-tree fruit stones," *Ecotox. Environ. Safe.* 84, 39-45. DOI: 10.1016/j.ecoenv.2012.06.019
- Albadarin, A. B., Ala'a H. Al-Muhtaseb, Al-Laqtah, N. A., Walker, G. M., Allen, S. J., and Ahmad, M. N. M. (2011). "Biosorption of toxic chromium from aqueous phase by lignin: Mechanism, effect of other metal ions and salts," *Chemical Engineering Journal* 169(1-3), 20-30. DOI: 10.1016/j.cej.2011.02.044
- Balakshin, M., Capanema, E., Gracz, H., Chang, H. M., and Jameel, H. (2011). "Quantification of lignin-carbohydrate linkages with high-resolution NMR spectroscopy," *Planta* 233(6), 1097-1110. DOI: 10.1007/s00425-011-1359-2
- Balea, A., Merayo, N., De La Fuente, E., Negro, C., and Blanco, Á. (2017). "Assessing the influence of refining, bleaching and TEMPO-mediated oxidation on the production of more sustainable cellulose nanofibers and their application as paper additives," *Ind. Crop Prod.* 97, 374-387. DOI: 10.1016/j.indcrop.2016.12.050
- Brdar, M., Šćiban, M., Takači, A., and Došenović, T. (2012). "Comparison of two and three parameters adsorption isotherm for Cr(VI) onto Kraft lignin," *Chem. Eng. J.* 183, 108-111. DOI: 10.1016/j.cej.2011.12.036
- Buranov, A. U., and Mazza, G. (2008). "Lignin in straw of herbaceous crops," *Ind. Crop Prod.* 28(3), 237-259. DOI: 10.1016/j.indcrop.2008.03.008
- Chao, L., Wenjun, L., Tiantian, L., Qi, Z., Haifeng, L., and Luru, J. (2018). "A study on adsorption of Cr(VI) by modified rice straw: Characteristics, performances and mechanism," *Journal of Cleaner Production* S095965261831638X-. DOI: 10.1016/j.jclepro.2018.05.279
- Faix, O. (1991). "Classification of lignins from different botanical origins by FT-IR spectroscopy," *Holzforschung* 45(s1), 21-28. DOI: 10.1515/hfsg.1991.45s1.21
- Fidalgo, M. L., Terron, M. C., Martinez, A. T., Gonzalez, A. E., Gonzalez-vila, F. J., and Galletti, G. C. (1993). "Comparative study of fractions from alkaline extraction of wheat straw through chemical degradation, analytical pyrolysis, and spectroscopic techniques," *J. Agr. Food Chem.* 41(10), 1621-1626. DOI: 10.1021/jf00034a019
- Ho, Y. S., and McKay, G. (1999). "Pseudo-second order model for sorption processes," *Process Biochem.* 34(5), 451-465. DOI: 10.1016/S0032-9592(98)00112-5
- Langmuir, I. (1916). "The constitution and fundamental properties of solids and liquids," *J. Am. Chem. Soc.* 38(9), 1848-1906. DOI: 10.1021/ja02254a006
- Li, M. F., Sun, S. N., Xu, F., and Sun, R. C. (2012). "Microwave-assisted organic acid extraction of lignin from bamboo: structure and antioxidant activity investigation," *Food Chem.* 134, 1392-398. DOI: 10.1016/j.foodchem.2012.03.037
- Ma, X., Long, Y., Duan, C., Lin, X., Cao, S., Chen, L., Huang, L., Ni, Y., Ma, X., and Long, Y. (2017). "Facilitate hemicelluloses separation from chemical pulp in ionic

- liquid/water by xylanase pretreatment,” *Ind. Crop. Prod.* 109, 459-463. DOI: 10.1016/j.indcrop.2017.08.063
- Meighan, B. N., Lima, D. R. S., Cardoso, W. J., Baêta, B. E. L., Adarme, O. F. H., Santucci, B. S., Pimenta, M. T. B., Aquino, S. F. D., and Gurgel, L. V. A. (2017). “Two-stage fractionation of sugarcane bagasse by autohydrolysis and glycerol organosolv delignification in a lignocellulosic biorefinery concept,” *Ind. Crop. Prod.* 108, 431-441. DOI: 10.1016/j.indcrop.2017.06.049
- Menezes, F. F. D., Fernandes, R. H. D. S., Rocha, G. J. D. M., and Filho, R. M. (2016). “Physicochemical characterization of residue from the enzymatic hydrolysis of sugarcane bagasse in a cellulosic ethanol process at pilot scale,” *Ind. Crop. Prod.* 94, 463-470. DOI: 10.1016/j.indcrop.2016.09.014
- Saleem, M., Aslam, F., Akhtar, M. S., Tariq, M., Rajoka, M. I. (2011). “Characterization of a thermostable and alkaline xylanase from *Bacillus* sp. and its bleaching impact on wheat straw pulp,” *World J. Microbiol. Biotechnol.* 28, 513-522. DOI: 10.1007/s11274-011-0842-z
- Saha, P., Chowdhury, S., Gupta, S., and Kumar, I. (2010). “Insight into adsorption equilibrium, kinetics and thermodynamics of Malachite Green onto clayey soil of Indian origin,” *Chem. Eng. J.* 165(3), 874-882. DOI: 10.1016/j.cej.2010.10.048
- Sasaki, K., Okamoto, M., Shirai, T., Tsuge, Y., Teramura, H., Sasaki, D., and Kikuchi, J. (2015). “Precipitate obtained following membrane separation of hydrothermally pretreated rice straw liquid revealed by 2D NMR to have high lignin content,” *Biotechnol. Biofuels* 8(1), 88. DOI: 10.1186/s13068-015-0273-4
- Scalbert, A., Monties, B., Lallemand, J.-Y., Guittet, E., and Rolando, C. (1985). “Ether linkage between phenolic acids and lignin fractions from wheat straw,” *Phytochemistry* 24(6), 1359-1362. DOI: 10.1016/S0031-9422(00)81133-4
- Scalbert, A., Monties, B., Rolando, C., and Sierra-Escudero, A. (1986). “Formation of ether linkage between phenolic acids and gramineae lignin: A possible mechanism involving quinone methides,” *Holzforschung* 40(3), 191-195. DOI: 10.1515/hfsg.1986.40.3.191
- Sindhu, R., Binod, P., and Pandey, A. (2016). “Biological pretreatment of lignocellulosic biomass - An overview,” *Bioresource Technology* 199, 76-82. DOI: 10.1016/j.biortech.2015.08.030
- Singh, R., Singh, S., Trimukhe, K. D., Pandare, K. V., Bastawade, K. B., Gokhale, D. V., and Varma, A. J. (2005). “Lignin-carbohydrate complexes from sugarcane bagasse: Preparation, purification, and characterization,” *Carbohydr. Polym.* 62(1), 57-66. DOI: 10.1016/j.carbpol.2005.07.011
- Sluiter, A., Hames, B., Ruiz, R., Scarlata, C., Sluiter, J., Templeton, D., and Crocker, D. (2008). *Determination of Structural Carbohydrates and Lignin in Biomass* (TP-510-42618), National Renewable Energy Laboratory, Golden, CO.
- Sun, S. L., Huang, Y., Sun, R. C., and Tu, M. B. (2016). “The strong association of condensed phenolic moieties in isolated lignins with their inhibition of enzymatic hydrolysis,” *Green. Chem.* 18, 4276-4286. DOI: 10.1039/C6GC00685J
- TAPPI. (1996). “TAPPI Test Methods 1996-1997,” TAPPI Press, Atlanta, GA, USA
- Tolbert, A., Akinosho, H., Khunsupat, R., Naskar, A. K., and Ragauskas, A. J. (2014). “Characterization and analysis of the molecular weight of lignin for biorefining studies,” *Biofuels, Bioproducts and Biorefining*, 8(6), 836-856. DOI: 10.1002/bbb.1500

- Toledano, A., Serrano, L., Garcia, A., Mondragon, I., and Labidi, J. (2010). "Comparative study of lignin fractionation by ultrafiltration and selective precipitation," *Chem. Eng. J.* 157(1), 93-99. DOI: 10.1016/j.cej.2009.10.056
- Wells, A., Teria, M., and Eve, T. (2006). "Green oxidations with laccase-mediator systems," *Biochemical Society Transactions* 34(2), 304. DOI: 10.1042/BST20060304
- Wörmeyer, K., Ingram, T., Saake, B., Brunner, G., and Smirnova, I. (2011). "Comparison of different pretreatment methods for lignocellulosic materials. Part II: Influence of pretreatment on the properties of rye straw lignin," *Bioresource Technol.* 102(5), 4157-4164. DOI: 10.1016/j.biortech.2010.11.063
- Wright, P. J., and Wallis, A. F. A. (1998). "Rapid determination of cellulose in plantation eucalypt woods to predict kraft pulp yields," *Tappi Journal* 81(2), 126-130. DOI: 10.1126/science.185.4153.791
- Yang, H.-T., Xie, Y.-M., Zheng, X., Pu, Y.-Q., Huang, F., Meng, X.-Z., Wu, W.-B., Ragauskas, A., and Yao, L. (2016). "Comparative study of lignin characteristics from wheat straw obtained by soda-AQ and kraft pretreatment and effect on the following enzymatic hydrolysis process," *Bioresource Technol.* 207, 361-369. DOI: 10.1016/j.biortech.2016.01.123
- Yang, H., Zheng, X., Yao, L., and Xie, Y. (2014). "Structural changes of lignin in the soda-AQ pulping process studied using the carbon-13 tracer method," *BioResources* 9(1), 176-190. DOI: 10.15376/biores.9.1.176-190
- Ying, W.-J., Shi, Z.-J., Yang, H.-Y., Xu, G.-F., Zheng, Z.-F., and Yang, J. (2018). "Effect of alkaline lignin modification on cellulase-lignin interactions and enzymatic saccharification yield," *Biotechnol. Biofuels* 11, 214. DOI: 10.1186/s13068-018-1217-6
- Yuan, T.-Q., He, J., Xu, F., and Sun, R.-C. (2009). "Fractionation and physico-chemical analysis of degraded lignins from the black liquor of *Eucalyptus pellita* KP-AQ pulping," *Polym. Degrad. Stab.* 94(7), 1142-1150. DOI: 10.1016/j.polymdegradstab.2009.03.019
- Zhang, L., Fu, F.-L., and Tang, B. (2019). "Adsorption and redox conversion behaviors of Cr(VI) on goethite/carbon microspheres and akaganeite/carbon microspheres composites," *Chem. Eng. J.* 356, 151-160. DOI: 10.1016/j.cej.2018.08.224
- Zhao, L.-S., Ouyang, X.-P., Ma, G.-F., Qian, Y., Qiu, X.-Q., and Ruan, T. (2018). "Improving antioxidant activity of lignin by hydrogenolysis," *Ind. Crop. Prod.* 125(1), 228-235. DOI: 10.1016/j.indcrop.2018.09.002
- Zikeli, F., Ters, T., Fackler, K., Srebotnik, E., and Li, J.-B. (2016). "Wheat straw lignin fractionation and characterization as lignin-carbohydrate complexes," *Ind. Crop. Prod.* 85, 309-317. DOI: 10.1016/j.indcrop.2016.03.012

Article submitted: January 21, 2019; Peer review completed: March 29, 2019; Revised version received: May 16, 2019; Accepted: May 17, 2019; Published: May 31, 2019. DOI: 10.15376/biores.14.3.5615-5629